

Modeling Short-term Yield Changes in Sweet Pepper Based on Dry Matter Production and Fruit Growth

Masaru Homma, Tadahisa Higashide, and Dong-Hyuk Ahn

Institute of Vegetable and Floriculture Science, National Agriculture and Food Research Organization, Kannonnai 3-1-1, Tsukuba, Ibaraki 305-8519, Japan

KEYWORDS. *Capsicum annuum*, crop model, dry matter fraction, flush, fruit growth curve

ABSTRACT. Large fluctuations in fruit set and fresh yield are issues associated with the production of sweet pepper. Fluctuations in fresh yield (i.e., flush) result in improper labor distributions and price fluctuations for growers. Modeling the fruit set is a promising way to improve the profits of growers and allow the arrangement of labor distribution and logistics. Therefore, this study aimed to develop a model for predicting the short-term yield changes of sweet pepper by integrating two sub-models: one model for predicting the production of total dry matter and one model for predicting the individual fruit growth. We hydroponically grew four sweet pepper cultivars (Artega, Nagano, Nesbitt, and Trirosso) in a greenhouse to investigate the accuracy of the proposed model. Comparisons between observed and predicted fresh yields showed that the peaks and troughs of fresh yields were accurately predicted, regardless of cultivar differences. The average root mean square error between them was within the range of 0.24 to 0.39 t·ha⁻¹·d⁻¹. Therefore, growers will be able to predict short-term yield changes of sweet pepper by obtaining coefficients for predicting the production of total dry matter and fruit growth curve of the cultivar scheduled to be cultivated.

Large fluctuations in fruit set and fresh yield are issues associated with the production of sweet pepper (*Capsicum annuum*), even when plants are grown in optimal environments (Homma et al. 2022; Ma et al. 2011). This phenomenon is called flush, and alternating high and low fresh yields are caused by high and low fruit sets, respectively (Abdel-Mawgoud et al. 2008; Al-Halimi and Moussa 2015; Heuvelink et al. 2004). Flushes are observed during the production of a broad range of greenhouse sweet pepper (Wien et al. 1989; Wubs et al. 2009a) and result in unstable fruit production for growers. In response to the peaks and troughs of fresh yields, a lack or excess of labor occurs during harvest times (Heuvelink et al. 2015). Simultaneously, periods of high market supply with low prices and periods of low market supply with high prices cyclically occur during production (Heuvelink et al. 2004).

Predicting short-term yield changes is a promising approach for resolving improper labor distribution and price fluctuations. For example, Sauviller et al. (2009) and Tijssens et al. (2004) reported that growers could optimize the labor force and logistics in advance of each harvest based on the data of predicted yields. Furthermore, Higashide (2018) and Sauviller et al. (2009) reported that sellers could arrange a preordered volume of fruits without lack or excess, thus stabilizing the negotiated unit price. Therefore, predicting short-term yield changes can improve labor efficiency and profitability.

For horticultural fruits and vegetables, some explanatory models that contain quantitative descriptions of internal mechanisms and processes of plants (Marcelis et al. 1998) have been developed to predict fresh yields. For example, some models consider yield components (Higashide 2018, 2022) and dynamic dry

matter partitioning to fruits (Heuvelink 1996; Marcelis 1994; Marcelis et al. 2006). The former model was based on photosynthesis and crop parameters (i.e., light extinction coefficient, efficiency of light usage, and dry matter fraction to fruits), and the latter was based on source-to-sink relationships. However, Wubs et al. (2009b) reported that the number of peaks and troughs of fresh yields were closely related to the fruit size of each cultivar. Therefore, modeling the growth of different fruits of each cultivar and incorporating it into the existing model has the potential to predict fresh yields with high accuracy.

This study aimed to develop a model for predicting the short-term fresh yield changes of sweet pepper. We constructed a model by coupling two sub-models: one model for predicting the production of dry matter and one model for predicting the individual fruit growth. The former sub-model was composed by considering yield components, and the latter one was composed by considering fruit growth curves. Environmental data of the greenhouse (e.g., air temperature, solar radiation) and plant growth data (e.g., leaf area index, fruit set) were used to calculate the sub-models. The presented model used these data for estimating fresh yields at least 1 to 30 d after the predicting date. To evaluate the accuracy of the proposed model, we grew four sweet pepper cultivars with different fruit sizes. Plants were grown using a hydroponic rockwool system in a greenhouse for 250 d, predicted and observed fresh yields were discussed, and model limitations and future implications were mentioned.

Materials and Methods

GROWING CONDITIONS. We hydroponically grew sweet pepper plants (cultivar Artega from Enza Zaden, Enkhuizen, the Netherlands; cultivars Nagano, Nesbitt, and Trirosso from Rijk Zwaan and Zuid-Holland, the Netherlands) in one small compartment of a Venlo-type greenhouse (width 18 m; length 18 m; height 5.1 m) in Tsukuba, Japan (lat. 36°26'N, long. 140°10'E, elevation 22 m). Sweet pepper seeds were sown in seed trays on 17 Jul 2020. The seeds were germinated in nursery soil and then grown under constant illumination with fluorescent lamps at a photosynthetic photon

Received for publication 28 Jul 2023. Accepted for publication 3 Oct 2023. Published online 12 Dec 2023.

We thank Takurou Nakayama, Toshiyuki Kurisaki, Takafumi Watabe, Yota Shinohara, and Masahide Isozaki of the Institute of Vegetable and Floriculture Science (NARO) for growing the plants and providing technical advice. D.-H.A. is the corresponding author. E-mail: ahn@affrc.go.jp. This is an open access article distributed under the CC BY-NC-ND license (<https://creativecommons.org/licenses/by-nc-nd/4.0/>).

flux density (PPFD) of 400 $\mu\text{mol}\cdot\text{m}^{-2}\cdot\text{s}^{-1}$, with a 16-h daytime (25 °C)/8-h nighttime (20 °C) cycle under a 1000 $\mu\text{mol}\cdot\text{mol}^{-1}$ CO₂ atmosphere in a growth chamber (Nae-terrace, 4–6T; Mitsubishi Chemical Agri Dream, Tokyo, Japan). We fertilized the seedlings every day with a commercial nutrient solution (High-Tempo; Sumitomo Chemical, Tokyo, Japan) at an adjusted electrical conductivity (EC) of 1.8 dS·m⁻¹. This solution consisted of 10.07 mmol nitrogen, 3.07 mmol phosphorus, 5.61 mmol potassium, 4.96 mmol calcium, 1.67 mmol magnesium, 0.34 mg·L⁻¹ manganese, 0.23 mg·L⁻¹ boron, 3.39 mg·L⁻¹ iron, 0.13 mg·L⁻¹ zinc, 0.04 mg·L⁻¹ copper, and 0.06 mg·L⁻¹ molybdenum. After 3 weeks, the seedlings were moved to the greenhouse and raised for 2 weeks in the secondary nursery.

On 20 Aug 2020, the seedlings were transplanted to rockwool cubes (7.5 × 7.5 × 6.5 cm; Grodan Delta Block; Rockwool B.V., Limburg, the Netherlands) and placed on rockwool slabs (100 × 20 × 7.5 cm; Grotop Expert; Grodan, Roermond, the Netherlands) in the greenhouse. The greenhouse was divided into five rows, and the inter-row and plant bed widths were approximately 1.8 and 0.6 m, respectively. Planting beds were arranged into a double-row planting system. A randomized complete block design was applied using two blocks with four plots. For each cultivar, 40 to 60 plants were transplanted to one plot, and a total of 396 plants were transplanted in the greenhouse ('Artega', 120 plants; 'Nesbitt', 98 plants; 'Nagano', 90 plants; and 'Trirosso', 88 plants). Plants on both sides were grown as guards for the three central rows. These guard plants were excluded from the measurements. The planting density was 3.7 plants/m². Plants were trained on two main stems, and the weak laterals of each dichotomous branch above the first leaf were pruned once per week.

The environmental conditions in the greenhouse were recorded and controlled every 5 min using an Integrated Environmental Controlling System (Maximizer; Priva. B.V., South Holland, the Netherlands). Irrigation and the CO₂ supply were controlled using a ubiquitous environmental controlling system (Hoshi et al. 2018). Ventilation windows were automatically opened when the air temperature in the greenhouse exceeded 28 °C [0–80 and 210–250 d after transplanting (DAT)]. The ventilation windows were closed from 81 to 209 DAT to maintain a highly concentrated CO₂ environment. The CO₂ concentration in the greenhouse was maintained by applying liquid CO₂. Daytime CO₂ concentrations at 42 to 80 and 81 to 209 DAT were maintained at 400 and 800 $\mu\text{mol}\cdot\text{mol}^{-1}$, respectively. From 210 to 250 DAT, daytime CO₂ concentrations were maintained at 400 $\mu\text{mol}\cdot\text{mol}^{-1}$.

A heat pump (Green Package, NGP104T-N; Nepon, Tokyo, Japan) was used for cooling at night when the air temperature in the greenhouse exceeded 20 °C until 0 to 56 DAT. The heat pump was also used for dehumidification when the relative air humidity in the greenhouse exceeded 75% at 81 to 209 DAT. A fogging system (LYOHM system, CoolPescon CH; Ikeuchi,

Tokyo, Japan) was used for maintaining the relative air humidity at 75% during the day. A heater (House Kaonki, HK2027TEN; Nepon) was set to turn on at 57 to 250 DAT when the air temperature dropped 18 °C at night (from sunset to sunrise) and 23 °C in the daytime (from sunrise to sunset). A shade curtain (SLS 50 Harmony; Svensson, Kinna, Sweden) was extended across the whole roof when the outside solar radiation reached 0.6 and 1.0 kW·m⁻² at 0 to 56 and 57 to 250 DAT, respectively.

The plants were supplied with commercial nutrient solution (OAT-SA; OAT Agrio, Tokyo, Japan). The EC of the nutrient solution was maintained at 1.8, 2.1, and 2.5 dS·m⁻¹ at 0 to 50, 51 to 80, and 81 to 250 DAT, respectively. The OAT-SA solution adjusted to an EC of 2.6 dS·m⁻¹ according to the manufacturer's instructions consisted of 21.5 mmol nitrogen, 4.4 mmol phosphorus, 10.2 mmol potassium, 4.1 mmol calcium, 1.5 mmol magnesium, 2.75 mg·L⁻¹ manganese, 3.05 mg·L⁻¹ boron, 7.95 mg·L⁻¹ iron, 0.07 mg·L⁻¹ copper, 0.17 mg·L⁻¹ zinc, and 0.07 mg·L⁻¹ molybdenum. The frequency of irrigation was controlled based on the outside solar radiation, and irrigation was performed every 0.6 to 0.8 MJ·m⁻² (0.4–2.8 L/plant/d). Drainage was discarded, and the daily drainage rate (drainage/supplied water) was maintained over 30%. The changes in environmental conditions are presented in Table 1. The daily average air temperature, daily average relative air humidity, and cumulative outside solar radiation and daytime average CO₂ concentration in the greenhouse calculated every 30 d were maintained within the range of 21 to 26 °C, 77% to 96%, 7.6 to 15.7 MJ·m⁻², and 380 to 760 $\mu\text{mol}\cdot\text{mol}^{-1}$, respectively.

MEASUREMENTS. For randomly selected plants in each plot at 0 DAT (a total of 8 plants of 'Nagano', 'Nesbitt', and 'Trirosso' and 12 plants of 'Artega'), the dates of anthesis and abortion at each node on the main stem during 0 to 230 DAT were continuously recorded twice per week. The dates of anthesis were defined as the days when the petals had completely opened, and pollen was considered to have been produced (Homma et al. 2022; Wubs et al. 2011). Mature fruits of the selected plants were regularly harvested once or twice per week until the end of cultivation; then, fruit fresh and dry weights (g/fruit) of each fruit were measured. Dry weights were measured after drying the fruits at 105 °C for at least 72 h using a ventilation drier (large forced ventilation drier, JMB-28DPN-S; Maruto Testing Machine Company, Tokyo, Japan). The numbers of harvested fruits of 'Artega', 'Nagano', 'Nesbitt', and 'Trirosso' during cultivation were approximately 341, 126, 132, and 269, respectively. We calculated the fruit dry matter content (g·g⁻¹) by dividing the dry weight by the fresh weight of fruit.

The leaf area index (LAI) (m²·m⁻²) and fresh and dry weights (g/plant) of each organ (stem, leaves, and fruits) were regularly measured during the experiment (for 'Artega': 0, 43, 106, 155, 196, and 250 DAT; for 'Nagano', 'Nesbitt', and 'Trirosso': 0, 79, 124, 190, and 244 DAT). Leaf area was measured using a leaf

Table 1. Average daily air temperature (Temp; °C), relative air humidity (Hmd; %), daytime CO₂ concentration (CO₂; $\mu\text{mol}\cdot\text{mol}^{-1}$), and cumulative outside solar radiation (SR; MJ·m⁻²) in the greenhouse every 30 d from 0 to 250 d after transplanting.

Environments	Unit	Days after transplanting								
		0–30	31–60	61–90	91–120	121–150	151–180	181–210	211–240	241–250
Temp	°C	25.9	22.3	22.0	21.5	21.0	21.4	22.4	22.6	22.9
Hmd	%	89.2	95.9	89.4	89.2	79.7	77.2	86.1	85.4	85.3
CO ₂	$\mu\text{mol}\cdot\text{mol}^{-1}$	383.4	407.7	488.8	756.7	749.1	733.2	687.8	420.3	407.8
SR	MJ·m ⁻²	15.7	8.3	10.3	7.6	8.9	10.6	14.4	15.5	21.7

area meter (LI-3100C; LI-COR, Lincoln, NE, USA). The LAI was calculated by multiplying the leaf area per plant (plant/m²) and planting density (3.7 plants/m²). Four plants in each plot (eight plants in total) were randomly sampled for ‘Artega’, and two plants (79, 124, and 190 DAT) and four plants (0 and 244 DAT) in each plot (four or eight plants in total) were randomly sampled for ‘Nagano’, ‘Nesbitt’, and ‘Trirosso’. Plants surrounding the sampled plants were excluded from subsequent measurements because they were grown with decreased plant density (<3.7 plants/m²).

Light extinction coefficient (*k*) was estimated according to Higashide (2022) and Watabe et al. (2021). The plant canopy was segmented into three layers [‘Artega’: 106 DAT (*n* = 8) and 250 DAT (*n* = 8); ‘Nagano’, ‘Nesbitt’, and ‘Trirosso’: 79 DAT (*n* = 4) and 244 DAT (*n* = 8)], and the PPFD in each layer was measured using a line quantum sensor (LI-191R; LI-COR) and a light meter (LI-250A; LI-COR). After PPFD measurements, the leaf area was individually measured to estimate the cumulative LAI of each layer. The light extinction coefficient (*k*) for each cultivar was obtained from the slope of the linear regression analysis curve using the relative PPFD and cumulative LAI in each layer (Monsi and Saeki 2005).

Dry weights of fruit (g/fruit) with different sizes were measured to determine the fruit growth curve. Dates of anthesis from 15 to 60 DAT (‘Nagano’, ‘Nesbitt’, and ‘Trirosso’) and 80 to 130 DAT (‘Artega’) for 20 to 30 plants were recorded for each cultivar after fixation of the fruit set. These tagged immature fruits [‘Nagano’ (*n* = 106), ‘Nesbitt’ (*n* = 74), and ‘Trirosso’ (*n* = 66)] were randomly sampled at 54, 61, 71, and 81 DAT. Similarly, tagged ‘Artega’ fruits (*n* = 101) were randomly sampled at 123, 140, 147, and 151 DAT.

MODEL DESCRIPTION. We compared two yield prediction models during this study. One model was in accordance with the work of Saito et al. (2020) and was developed to predict fresh tomato yields based on Eqs. [1] to [5] (model 1). Another model presented in this study was based on Eqs. [1] to [3] and Eqs. [5] to [12] (model 2). The flow diagram of the fresh yield prediction is shown in Fig. 1. Using model 1 and model 2, the daily production of total dry matter and fresh yields were calculated using the same equations (Eqs. [1] to [3] and Eq. [5]) and the same coefficients (Fig. 1). We assumed that daily production of total dry matter was partitioned into fruits within 1 d (Yoshioka et al. 1977). Calculations for both models were performed on a daily basis.

MODEL 1. Daily production of total dry matter per unit area (DM; g·m⁻²·d⁻¹) was predicted. The DM at *m* DAT (DM_{*m*}) was predicted based on Eqs. [1] to [3] according to the calculation presented by Higashide (2022) and Saito et al. (2020):

$$DM_m = LUE_m \times IL_m \quad [1]$$

$$LUE_m = m \times \ln(CO_{2m}) + o \quad [2]$$

$$IL_m = (1 - e^{-k \times LAI_m}) \times T_g \times R_p \times Sr_m \quad [3]$$

where LUE_{*m*} (g·MJ⁻¹) is the efficiency of using light at *m* DAT. LUE_{*m*} is a function of the daytime CO₂ concentration in the greenhouse at *m* DAT (CO_{2*m*}, μmol·mol⁻¹). The coefficients (*m*, *o*) for estimating LUE_{*m*} were obtained from Homma et al. (2024) (*m* and *o*: ‘Artega’, 2.09 and -9.12; ‘Nagano’, 3.05 and -15.52; ‘Nesbitt’, 3.79 and -19.73; ‘Trirosso’, 4.25 and -22.35). IL_{*m*} (MJ·m⁻²·d⁻¹) is the cumulative amount of light intercepted by plants canopy at *m* DAT. IL_{*m*} is the function of outside solar radiation at *m* DAT (Sr_{*m*}; MJ·m⁻²·d⁻¹), light transmissivity of the greenhouse (T_{*g*}; 0.45 MJ·MJ⁻¹, measured before the

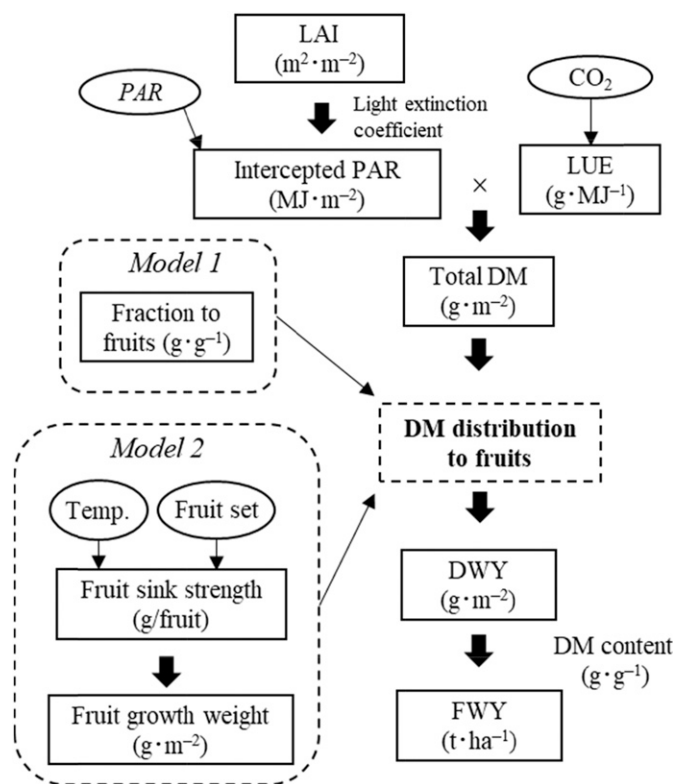


Fig. 1. A flow diagram for predicting fresh weight yields of sweet pepper grown in the greenhouse. DM = dry matter; DWY = dry weight yield; FWY = fresh weight yield; LAI = leaf area index; LUE = light use efficiency; PAR = photosynthetically active radiation; Temp. = daily average air temperature.

experiment), ratio of photosynthetically active radiation (*PAR*) to outside solar radiation (R_p ; $0.5 \text{ MJ}\cdot\text{MJ}^{-1}$) (Ohtani 1997), LAI at *m* DAT (LAI_m ; $\text{m}^2\cdot\text{m}^{-2}$), and light extinction coefficient (*k*, dimensionless). The LAI_m was estimated using a regression equation between the measured LAI and DAT ($R^2 = 0.98\text{--}0.99$). Regressive equations and parameters were observed as follows: ‘Artega’, $\text{LAI}_m = -0.000054 \times \text{DAT}^2 + 0.058 \times \text{DAT} + 0.47$; ‘Nagano’, $\text{LAI}_m = -0.00011 \times \text{DAT}^2 + 0.062 \times \text{DAT} + 0.39$; ‘Nesbitt’, $\text{LAI}_m = 0.019 \times \text{DAT} + 1.01$; and ‘Trirosso’, $\text{LAI}_m = 0.015 \times \text{DAT} + 0.47$. The light extinction coefficient (*k*) for estimating IL_m was obtained from the dataset described in the Measurements section (*k*: ‘Artega’, 0.55; ‘Nagano’, 0.58; ‘Nesbitt’, 0.57; ‘Trirosso’, 0.56). Dry weight yields at *m* DAT per unit area (DWY_m ; $\text{g}\cdot\text{m}^{-2}\cdot\text{d}^{-1}$) were calculated as follows:

$$\text{DWY}_m = \text{DM}_m \times F_f \quad [4]$$

where F_f ($\text{g}\cdot\text{g}^{-1}$) is a daily dry matter fraction of fruits, which was obtained from Table 2 (F_f : ‘Artega’, $0.48 \text{ g}\cdot\text{g}^{-1}$; ‘Nagano’, $0.54 \text{ g}\cdot\text{g}^{-1}$; ‘Nesbitt’, $0.47 \text{ g}\cdot\text{g}^{-1}$; and ‘Trirosso’, $0.49 \text{ g}\cdot\text{g}^{-1}$). Fresh weight yields at *m* DAT per unit area (FWY_m ; $\text{t}\cdot\text{ha}^{-1}\cdot\text{d}^{-1}$) were calculated as follows:

$$\text{FWY}_m = \frac{\text{DWY}_m}{\text{Cd} \times 100} \quad [5]$$

where Cd ($\text{g}\cdot\text{g}^{-1}$) is the dry matter content of fruit (Cd: ‘Artega’, $0.081 \text{ g}\cdot\text{g}^{-1}$; ‘Nagano’, $0.077 \text{ g}\cdot\text{g}^{-1}$; ‘Nesbitt’, $0.078 \text{ g}\cdot\text{g}^{-1}$; and ‘Trirosso’, $0.11 \text{ g}\cdot\text{g}^{-1}$), which was obtained from the dataset described in the Measurements section.

MODEL 2. Dry weights of fruits increased as a sigmoid function with increasing cumulative daily average air temperatures after anthesis (Wubs et al. 2012); therefore, we applied the Gompertz function (Eq. [6]) to estimate the dry weights of fruits. This function represents the relationship between the cumulative daily average air temperature after anthesis (CT, $^\circ\text{C}\cdot\text{d}$) and dry weight of fruit (DWF; g/fruit):

$$\text{DWF} = A \times b^{e^{-c \times \text{CT}}} \quad [6]$$

where the coefficients, A, b, and c, represent an upper asymptote line (g/fruit), intercept of the function (dimensionless), and constant determination of the curvature ($1/^\circ\text{C}\cdot\text{d}$), respectively. Differentiated fruit growth curves in Eq. [6] and the coefficients obtained during this experiment are shown in Fig. 2. Normalized fruit growth function (RFDWF ; $\text{g}\cdot\text{g}^{-1}$) was calculated as follows:

$$\text{RFDWF} = \frac{\text{DWF}}{A} \quad [7]$$

The potential daily increase in dry weight of growing fruit *j* at *m* DAT ($\text{pDWF}_{m,j}$; $\text{g}/\text{fruit}/\text{d}$) was calculated as follows:

$$\text{pDWF}_{m,j} = F_{\text{max}} \times (\text{RFDWF}_{m,j} - \text{RFDWF}_{m-1,j}) \quad [8]$$

where F_{max} (g/fruit) represents the growth potential of fruits by their dry weights. We defined F_{max} as the harvested heaviest fruit, which was obtained from the harvest survey as described in the Measurements section (F_{max} : ‘Artega’, $15.8 \text{ g}/\text{fruit}$; ‘Nagano’, $17.7 \text{ g}/\text{fruit}$; ‘Nesbitt’, $20.2 \text{ g}/\text{fruit}$; and ‘Trirosso’, $12.4 \text{ g}/\text{fruit}$). The potential daily dry matter distribution of fruits at *m* DAT (pDM_m ; $\text{g}\cdot\text{m}^{-2}\cdot\text{d}^{-1}$) was calculated as follows:

$$\text{pDM}_m = \alpha \times \text{DM}_m \quad [9]$$

where α is the partitioning coefficient ($\text{g}\cdot\text{g}^{-1}$). We set this coefficient to $0.70 \text{ g}\cdot\text{g}^{-1}$, according to Heuvelink (1997), Marcelis (1996), and Wubs (2010). These studies investigated the dry matter partitioning to fruits and organs for tomato, cucumber, and sweet pepper, and the α values ranged from approximately 0.60 to $0.80 \text{ g}\cdot\text{g}^{-1}$. We hypothetically set the α values as $0.70 \text{ g}\cdot\text{g}^{-1}$ to express the average. The production of the total dry matter per unit area at *m* DAT (DM_m ; $\text{g}\cdot\text{m}^{-2}\cdot\text{d}^{-1}$) was calculated using Eqs. [1] to [3], the actual daily increase in dry weight of fruit *j* at *m* DAT ($\text{acDW}_{m,j}$ $\text{g}/\text{fruit}/\text{d}$; Eq. [11]) was determined based on the daily calculated ratio of pDM_m to total $\text{pDWF}_{m,j}$ per unit area (β_m ; $\text{g}\cdot\text{g}^{-1}$; Eq. [10]). The subscript *j* represents the number of growing fruits per unit area at *m* DAT (fruits/m^2). Furthermore, β_m represents the internal competition for daily production of total dry matter between fruits and other organs. This coefficient was developed based on the concept of Marcelis et al. (2006) and Marcelis (1994). The difference in the β_m from the previous study was that without containing the functions for predicting vegetative growth.

$$\beta_m = \frac{\text{pDM}_m}{\sum_{j=0}^j \text{pDWF}_{m,j}} \quad [10]$$

We hypothesized that when β_m was greater than $1.0 \text{ g}\cdot\text{g}^{-1}$, pDM_m was partitioned to each fruit equal to the amount of $\text{pDWF}_{m,j}$. Additionally, we hypothesized that when β_m was less than $1.0 \text{ g}\cdot\text{g}^{-1}$, pDM_m was proportionally partitioned to each fruit according to the relative fruit sink strength (Marcelis 1994) as follows:

$$\text{acDW}_{m,j} = \begin{cases} \text{pDWF}_{m,j} & \beta_m > 1.0 \\ \beta_m \times \text{pDWF}_{m,j} & \beta_m \leq 1.0 \end{cases} \quad [11]$$

Dry weight yields at *m* DAT per unit area (DWY_m ; $\text{g}\cdot\text{m}^{-2}\cdot\text{d}^{-1}$) were calculated as follows:

Table 2. Average leaf area index (LAI; $\text{m}^2\cdot\text{m}^{-2}$), intercepted amount of light per plant canopy (IL; $\text{MJ}\cdot\text{m}^{-2}$), observed total dry matter production (Observed TDM; $\text{g}\cdot\text{m}^{-2}$), predicted total dry matter production (Predicted TDM; $\text{g}\cdot\text{m}^{-2}$), and dry matter fraction to each organ ($\text{g}\cdot\text{g}^{-1}$) of four sweet pepper cultivars grown in the greenhouse.

CV	DAT (d)	LAI ($\text{m}^2\cdot\text{m}^{-2}$)	IL ⁱ ($\text{MJ}\cdot\text{m}^{-2}$)	Observed TDM ($\text{g}\cdot\text{m}^{-2}$)	Predicted TDM ($\text{g}\cdot\text{m}^{-2}$)	Dry matter fraction ($\text{g}\cdot\text{g}^{-1}$)		
						Leaf	Stem	Fruit
AT	250	12.1 ⁱⁱ a ⁱⁱⁱ	596.6	2603 ± 181 a	2300	0.24 a	0.28 a	0.48 b
NG	244	9.2 b	567.1	1901 ± 162 b	2007	0.22 ab	0.24 b	0.54 a
NS	244	10.9 a	567.7	2066 ± 155 ab	2251	0.24 a	0.29 a	0.47 b
TR	244	8.6 b	533.8	2144 ± 215 ab	2283	0.20 b	0.31 a	0.49 b

ⁱ Cumulative values from transplanting to the end of cultivation are presented.

ⁱⁱ Average values are shown except for IL ($n = 8$). The observed TDM was shown as the average an *SD*.

ⁱⁱⁱ Different letters indicate significant differences ($n = 8$). ($P < 0.05$ according to Tukey’s multiple comparison test).

AT = Artega; CV = cultivar; DAT = days after transplanting; NG = Nagano; NS = Nesbitt; TR = Trirosso.

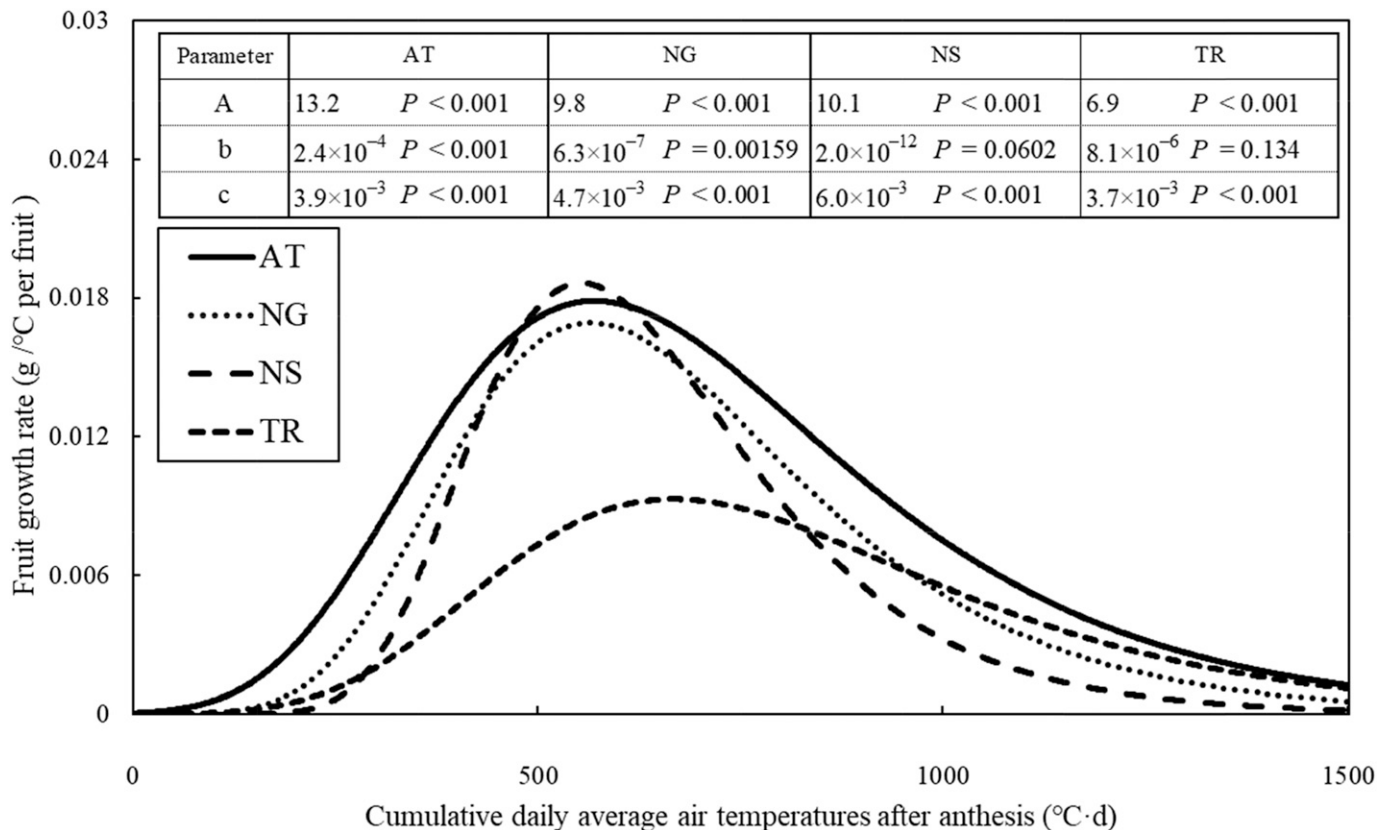


Fig. 2. Relationship between the cumulative daily average air temperatures after anthesis ($^{\circ}\text{C}\cdot\text{d}$) and estimated fruit growth rate ($\text{g}/^{\circ}\text{C}$ per fruit) of four sweet pepper cultivars grown in the greenhouse. AT, NG, NS, and TR represent the cultivars Artega, Nagano, Nesbitt, and Trirosso, respectively. Dry weights of the fruits were estimated by applying the Gompertz function (Eq. [6]). Coefficients (A, b, and c) of the Gompertz function were estimated using nonlinear regression analysis (AT: $n = 101$; NG: $n = 106$; NS: $n = 74$; TR: $n = 66$).

$$\text{DWY}_m = \sum_{j=0}^j \sum_{m=ad}^{m=hd} ac\text{DW}_{m,j} \quad \text{CT} > 1,200 \quad [12]$$

where ad and hd denote the dates of anthesis and harvest of the growing fruit j , respectively. We defined that fruits were harvested when the CT of fruit j reached $1200^{\circ}\text{C}\cdot\text{d}$ (i.e., cumulative daily average of the air temperature values after anthesis until harvest). The DWY_m was calculated by accounting for the harvestable fruits j (CT reached $1200^{\circ}\text{C}\cdot\text{d}$) per unit area. Fresh weight yields at m DAT per unit area (FWY_m ; $\text{t}\cdot\text{ha}^{-1}\cdot\text{d}^{-1}$) were calculated using Eq. [5]. Coefficient C_d in model 2 was the same as that in model 1.

STATISTICAL ANALYSIS. To validate the output of both models, we calculated the root mean square error (RMSE; $\text{t}\cdot\text{ha}^{-1}\cdot\text{d}^{-1}$) between the weekly moving averages of daily observed and estimated fresh weight yields. Additionally, we calculated the predicted cumulative FWY_m at the end of cultivation for both models and compared them with the observed ones. Statistical software (R version 3.6.3) (R Core Team 2020) was used for all statistical analyses.

Results

Predicted and observed TDM, observed LAI, estimated IL, and dry matter fraction of each organ at the end of cultivation are shown in Table 2. The observed LAI and estimated IL in each cultivar at the end of cultivation were more than $8.5 \text{ m}^2\cdot\text{m}^{-2}$ and $530 \text{ MJ}\cdot\text{m}^{-2}$, respectively (Table 2). Most of the estimated

cumulative TDM_m values were within the range of SDs of the observed TDM during cultivation (Table 2). The dry matter fraction of fruits at the end of cultivation was highest for ‘Nagano’, and no significant differences were observed among those for ‘Artega’, ‘Nesbitt’, and ‘Trirosso’ (Table 2). The dry matter fraction of fruits was valued within 0.47 to $0.54 \text{ g}\cdot\text{g}^{-1}$ (Table 2).

The differential curves of the Gompertz function obtained from randomly sampled fruit data indicated that most obtained parameters of the curves were statistically significant ($P \leq 0.05$). Dry weights of fruits increased from anthesis ($0^{\circ}\text{C}\cdot\text{d}$) until harvest (approximately 1200 to $1300^{\circ}\text{C}\cdot\text{d}$); however, the rate of increase was different for each cumulative temperature. For example, peaks of the rate of increase were observed between 500 and $700^{\circ}\text{C}\cdot\text{d}$, regardless of the cultivars (see the convex of each curve in Fig. 2). Coefficient A (described in Eq. [6]) was low for ‘Trirosso’ (A, $6.9 \text{ g}/\text{fruit}$; Fig. 2) compared with those of the other cultivars (A, 9.8 – $13.2 \text{ g}/\text{fruit}$; Fig. 2). This coefficient indicates fruit weight at the mature stage. The instantaneous rate of fruit growth for ‘Artega’, ‘Nesbitt’, and ‘Nagano’ reached 0.017 to $0.019 \text{ g}/^{\circ}\text{C}$ per fruit at the peak growth (approximately $600^{\circ}\text{C}\cdot\text{d}$); however, that of ‘Trirosso’ reached only $0.010 \text{ g}/^{\circ}\text{C}$ per fruit at the peak growth (approximately $700^{\circ}\text{C}\cdot\text{d}$) (see the convex of each curve in Fig. 2).

The changes of daily predicted production of the total dry matter during the experiment showed marked fluctuations (Fig. 3). These fluctuations partly corresponded to the fluctuations of outside solar radiation and the increase of the intercepted amount of

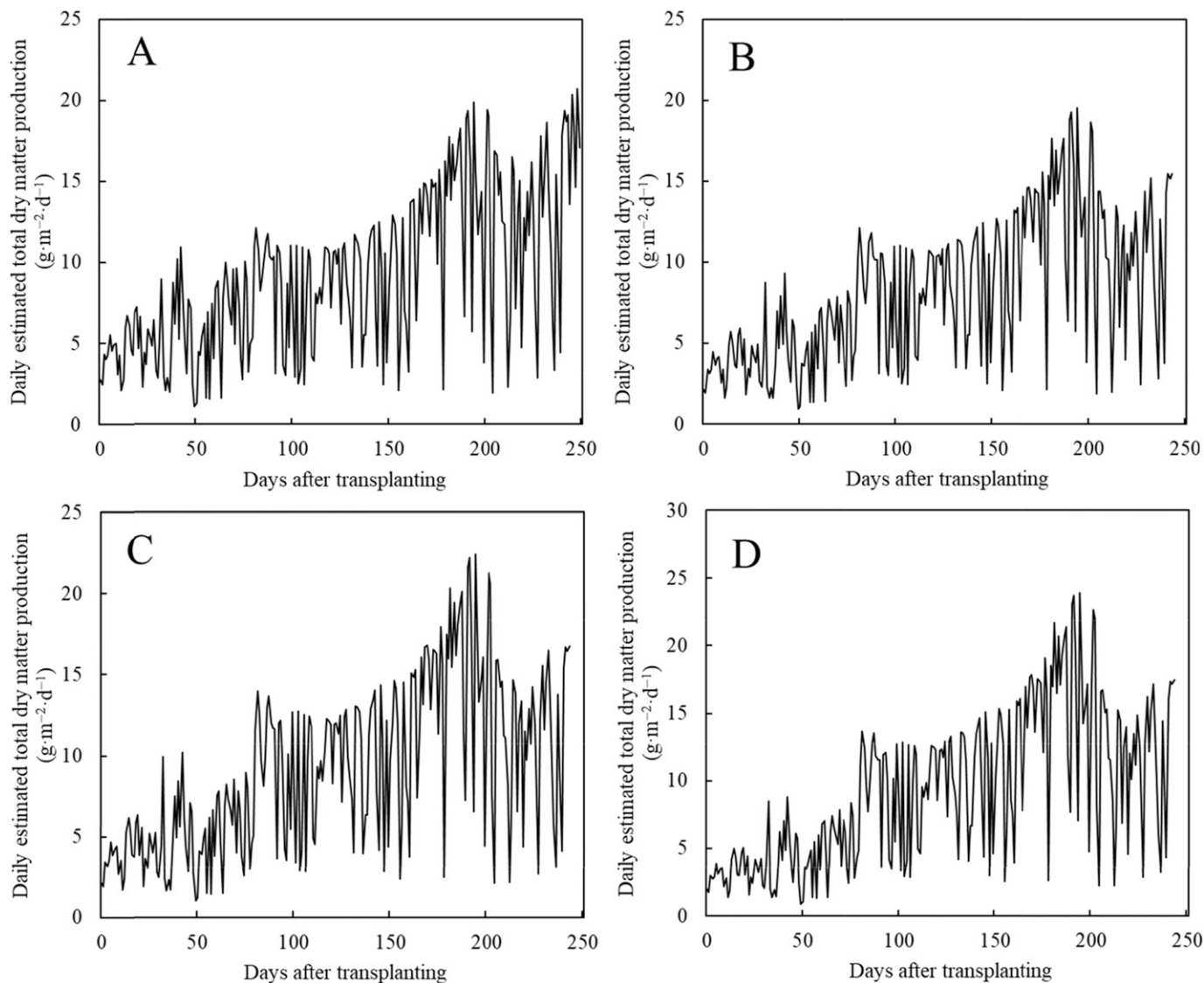


Fig. 3. Changes in the estimated daily total dry matter production ($\text{g}\cdot\text{m}^{-2}\cdot\text{d}^{-1}$) of four sweet pepper cultivars grown in the greenhouse from 0 to 250 d after transplanting. (A) 'Artega'. (B) 'Nagano'. (C) 'Nesbitt'. (D) 'Trirosso'.

light per plant canopy (data not shown). In other words, the predicted production of dry matter showed high and low values on sunny and rainy day, respectively. The predicted values of the total dry matter gradually increased until 200 DAT in response to the increment of LAI (Fig. 3); thereafter, the values decreased in response to the decrease of the daytime CO_2 concentration in the greenhouse (Table 1).

Daily fruit set fluctuations are shown in Fig. 4. Daily changes in the β_m showed that these values less than $1.0 \text{ g}\cdot\text{g}^{-1}$ were frequently observed for all cultivars during the experiment (Fig. 5). This result indicates that the plants canopy lacked sufficient photosynthates for fruit dry matter growth on rainy or cloudy days with little solar radiation. From 0 to 50 DAT, most of the β_m values were more than $1.0 \text{ g}\cdot\text{g}^{-1}$ (Fig. 5) because the number of fruit sets was small during this period (Fig. 4). However, the β_m values at approximately 150 and 210 DAT were almost less than $1.0 \text{ g}\cdot\text{g}^{-1}$ for all cultivars (Fig. 5). This decrease mainly resulted from the rapid increase of the fruit set at 110 and 170 DAT (Fig. 4) and the rapid increase of the fruit dry matter weight at

30 to 40 d (approximately $600\text{--}800^\circ\text{C}\cdot\text{d}$ after anthesis; Fig. 2) after the fruit set.

The changes in the observed number of fruits set on the day showed marked fluctuations (Fig. 4). For example, all cultivars showed peaks of the fruit set at approximately 30 to 40, 60 to 70, 90, 120, and 170 DAT. In contrast, they showed valleys of the fruit set at approximately 40, 60, 90 to 100, 140, and 180 to 200 DAT. The cumulative amount of fruit set during the experiment was highest and lowest for 'Trirosso' and 'Nesbitt', respectively (Fig. 4). By focusing on the fluctuations of fresh weight yields (Fig. 6), it was observed that most yield fluctuations occurred approximately 50 d after fluctuations of fruit set (Fig. 4). This delay resulted from the fruit ripening period; in other words, approximately 50 to 60 d (i.e., $1100\text{--}1200^\circ\text{C}\cdot\text{d}$ after anthesis; Eq. [12] and Fig. 2) was necessary for maturing when the daily average air temperature was maintained at 21 to 26°C (Table 1).

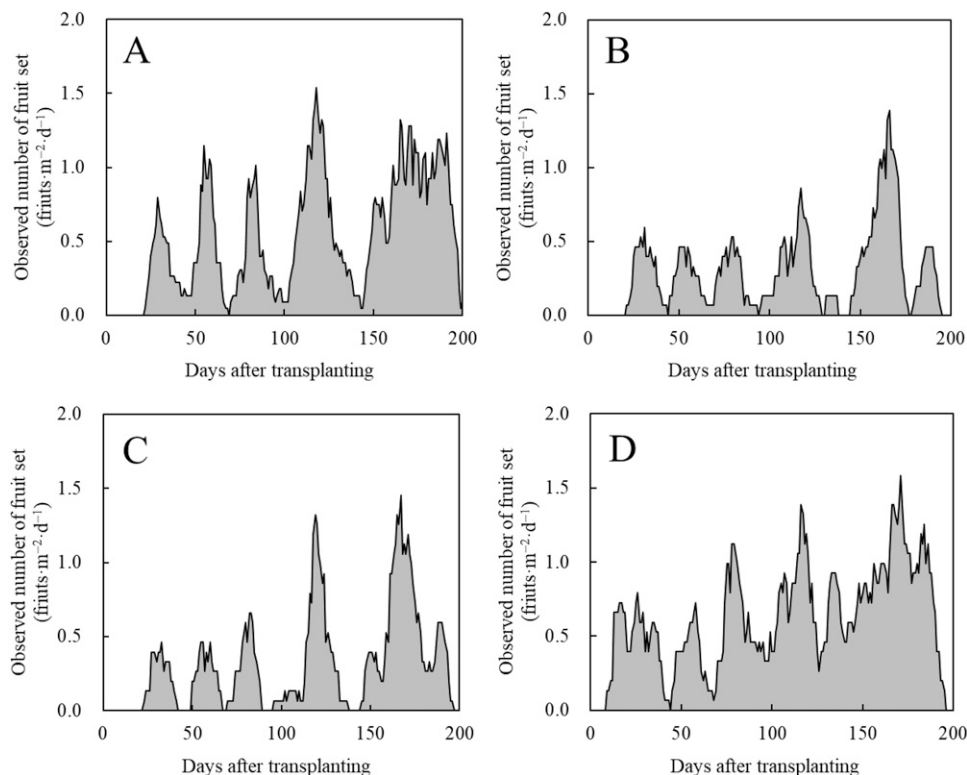


Fig. 4. Changes in the observed daily fruit set ($\text{fruits}\cdot\text{m}^{-2}\cdot\text{d}^{-1}$) of four sweet pepper cultivars grown in the greenhouse from 0 to 200 days after transplanting. (A) 'Artega'. (B) 'Nagano'. (C) 'Nesbitt'. (D) 'Trirosso'. The daily fruit set were shown as weekly moving averages from 12 ('Artega') and 8 ('Nagano', 'Nesbitt', and 'Trirosso') plants.

We presented the daily predicted and observed fresh weight yields during this experiment using equations from model 1 and model 2 (Fig. 6). Cyclic fluctuations in fresh weight yields were observed for each cultivar (see arrow symbols in Fig. 6). Peaks in the daily fresh weight yields were observed at approximately 80, 110, 140, 170, and 220 DAT. Additionally, troughs in the daily fresh weight yields were observed at approximately 100, 120, 150, 200, and 240 DAT. The peaks and troughs of the fresh weight yields almost coincided without depending on cultivars; however, the extent differed among cultivars (Fig. 6). For example, fluctuations in fresh weight yields were smaller for 'Trirosso' than those for other cultivars. Daily fresh weight yields of 'Nesbitt' and 'Nagano' fluctuated between 0 and $0.28 \text{ t}\cdot\text{ha}^{-1}\cdot\text{d}^{-1}$, and those of 'Trirosso' fluctuated between 0 and $0.14 \text{ t}\cdot\text{ha}^{-1}\cdot\text{d}^{-1}$.

The predicted fresh weight yields from model 2 showed cyclic patterns that were similar to the observed patterns, regardless of the cultivars (Fig. 6). For example, small and large fluctuations in fresh weight yields for 'Trirosso' and 'Nesbitt' were accurately predicted (Fig. 6). However, the predicted fresh weight yields from model 2 showed some overestimations and underestimations. First, the prediction shifted before and after the peaks of harvest (Fig. 6) ('Artega', 90 and 180 DAT; 'Trirosso', 180 DAT; 'Nagano', 110 and 220 DAT; and 'Nesbitt', 140 and 180 DAT). Next, improper estimations were observed during some periods (Fig. 6) ('Artega', 110 DAT; 'Trirosso', 140 DAT; 'Nagano', 110 DAT; and 'Nesbitt', 110 and 140 DAT). Overall, the calculated RMSE of the predicted fresh weight yields from model 1 and model 2 were within the ranges of 0.26 to 0.48 and 0.24 to $0.39 \text{ t}\cdot\text{ha}^{-1}\cdot\text{d}^{-1}$, respectively (Fig. 6).

The predicted and observed cumulative fresh weight yields at the end of cultivation are shown in Table 3. According to the values obtained by model 1, the predicted fresh weight yields of 'Nagano' and 'Trirosso' were within the range of the *SD* calculated from the observed values, but those of 'Artega' and 'Nesbitt' showed different trends (Table 3). The predicted fresh weight yields of 'Artega', 'Nagano', and 'Trirosso' from model 2 were within the range of the *SD* calculated from those observed, but those of 'Nesbitt' showed different trends (Table 3). Overall, when focusing on the cumulative fresh weight yields, model 1 and model 2 showed good predictions for 'Nagano' and 'Trirosso'. Only model 2 showed good predictions for 'Artega'. Model 1 and model 2 did not show good predictions for 'Nesbitt'.

The daily changes in the differences in the observed and predicted fruit fresh yields (dashed line for model 1 and solid line model 2 in Fig. 7) showed mispredictions for the outputs of both presented models. Although model 2 succeeded to predict the peaks and the valleys of yield fluctuations (Fig. 6), slight mispredictions of the harvest date (e.g., 210 DAT for 'Nagano' and 180 DAT for 'Nesbitt') (Fig. 6) resulted in the marked misprediction of fruit fresh weight (Fig. 7). Misprediction of the harvest date was closely related to the decreasing trend and fluctuation of the fruit maturing period (Table 4).

The cumulative values of the daily average air temperature after anthesis until harvest (CT, $^{\circ}\text{C}\cdot\text{d}$) were approximately 1120 to 1220 $^{\circ}\text{C}\cdot\text{d}$ for all cultivars; however, it showed a decreasing trend during cultivation (Table 4). For example, CT during 51 to 100 DAT was approximately 1240 to 1320 $^{\circ}\text{C}\cdot\text{d}$, but that during 201 to 250 DAT was approximately 1080 to 1165 $^{\circ}\text{C}\cdot\text{d}$.

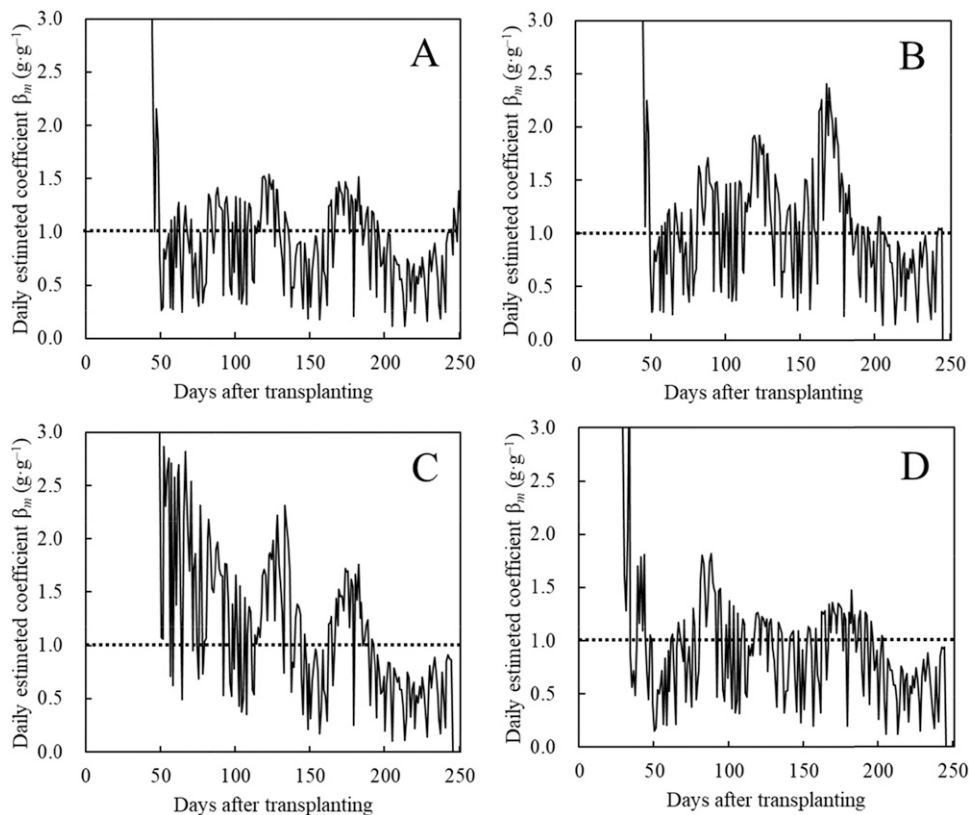


Fig. 5. Changes in the estimated daily coefficient β_m ($\text{g}\cdot\text{g}^{-1}$) of four sweet pepper cultivars grown in the greenhouse from 0 to 250 d after transplanting. These daily coefficients, β_m , were calculated by dividing the daily potential of dry matter distribution to fruits ($\text{g}\cdot\text{m}^{-2}$) by the fruit dry matter growth ($\text{g}\cdot\text{m}^{-2}$). β_m represents internal competition for the daily production of total dry matter between fruits and other organs. (A) 'Artega'. (B) 'Nagano'. (C) 'Nesbitt'. (D) 'Trirosso'.

Additionally, CT showed an *SD* of approximately 100 to 160 °C·d, irrespective of the cultivars (Table 4). These results indicate that the harvest period decreased by approximately 5 d during 0 to 250 DAT, and that it also fluctuated within the range of 5 to 8 d when plants were grown at a daily average air temperature of 20 °C.

Discussion

Similar to other horticultural crops such as tomato (*Solanum lycopersicum*) and cucumber (*Cucumis sativus*), sweet pepper is characterized by large fluctuations in the fruit set and fresh weight yields (Higashide 2009; Marcelis 1994; Marcelis et al. 2006). For sweet pepper, this might be closely related to the cyclic fluctuation in dry matter partitioning to vegetative and generative organs (Homma et al. 2022, 2024). Additionally, the number of peaks and amplitude of fluctuations in fresh weight yields are different in cultivars with different fruit sizes (Wubs et al. 2009b). Therefore, this study developed sub-models (Eqs. [6] to [12]) (Fig. 1) to calculate the daily process of dry matter partitioning to fruits by considering the cultivar's peculiar fruit size and fruit set. Additionally, this study predicted the daily production of total dry matter by considering the yield components according to previous reports (Fig. 3) (Eqs. [1] to [3]) (Higashide 2022; Saito et al. 2020; Watabe et al. 2021). By combining both, we proposed the model for predicting the short-term yield changes by adding a sub-model (Eqs. [6] to [12]) to the model presented by Higashide (2022) and Saito et al. (2020) (Eqs. [1] to

[5]). Overall, fluctuating short-term yield changes were accurately predicted (Fig. 6, Table 3) by imitating the daily process of producing total dry matter and its partitioning to fruits organs (Figs. 3 and 5) (Eqs. [1] to [3] and Eqs. [5] to [12]).

Fluctuations in the fresh weight yield of sweet pepper have been reported to be closely related to the following three major factors: assimilate supply (Homma et al. 2022), fruit load (Wien et al. 1989), and fruit size (Wubs et al. 2009b). During this study, the assimilate supply was calculated as the production of the total dry matter by considering the yield components (Eqs. [1] to [3]) (Higashide 2022; Saito et al. 2020). Next, the fruit load and fruit size were calculated as the increase in the dry weight of fruits by considering the actual fruit set and fruit growth curves (Figs. 2 and 4) (Eqs. [6] to [12]). The obtained fruit growth curve had its own fruit growth rate; there was a small growth rate for 'Trirosso' and a large growth rate for other cultivars (Fig. 2). Each cultivar had its own coefficients that represented individual fruit growth (Gompertz function: A, b, and c in Eq. [6]). Our model showed excellent prediction of yield changes for large fruit cultivars with remarkable fluctuations in the yield ('Nesbitt' and 'Nagano') and for small fruit cultivars with low fluctuations in the yield ('Trirosso') (Fig. 6, Table 3). As a result, fresh weight yields were accurately predicted, and this result was in agreements with those of previous reports (Al-Halimi and Moussa 2015; Lin and Hill 2008; Lin et al. 2009; Verlinden et al. 2005).

Yield changes predicted using model 1 showed high prediction accuracy for tomato (Saito et al. 2020) and cucumber (Maeda and Ahn 2021), although the accuracy was low for

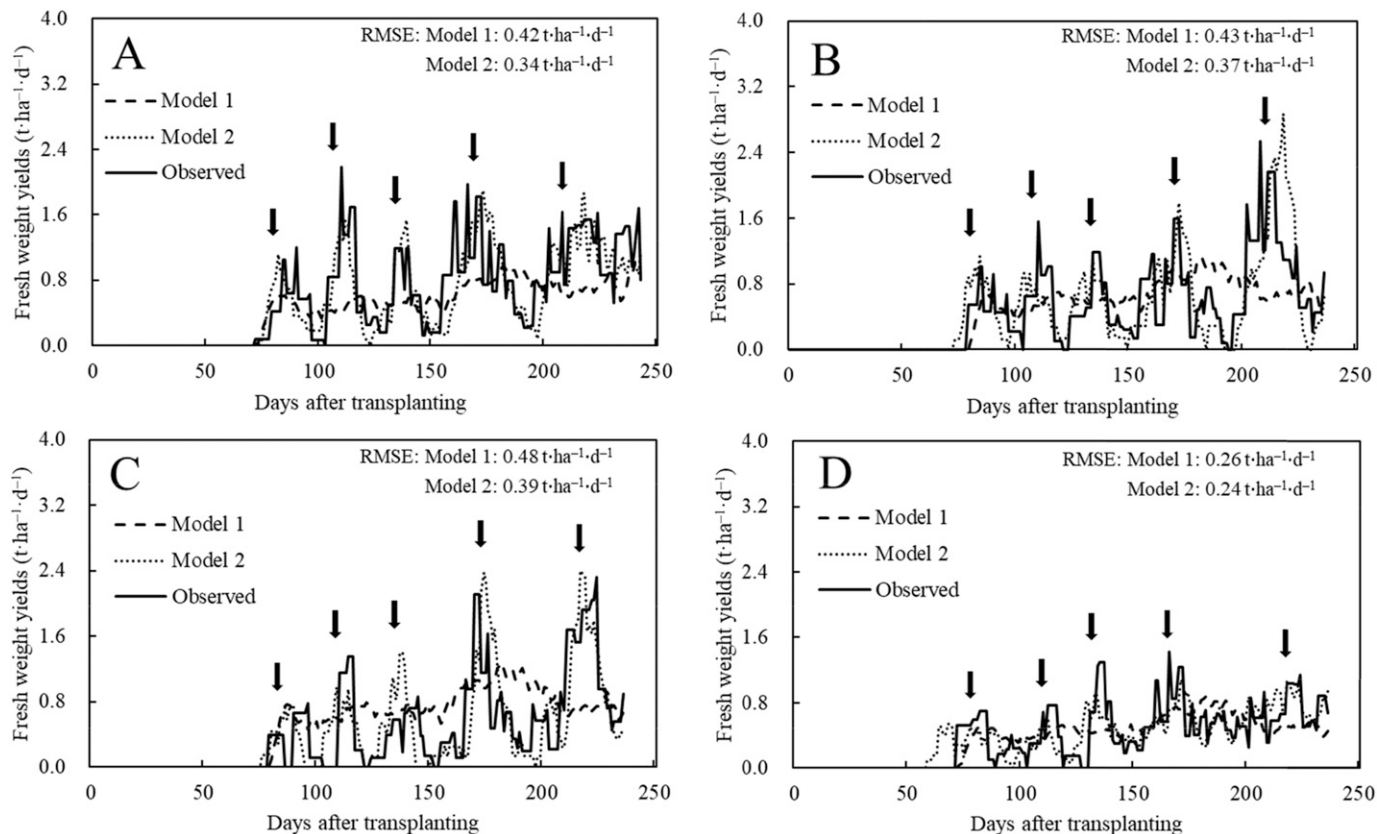


Fig. 6. Changes in the observed (solid line) and estimated (model 1: dashed line; model 2: dotted line) daily fresh weight yields ($t\cdot ha^{-1}\cdot d^{-1}$) of four sweet pepper cultivars grown in the greenhouse from 0 to 250 d after transplanting. (A) ‘Artega’. (B) ‘Nagano’. (C) ‘Nesbitt’. (D) ‘Trirosso’. Fresh weight yields are shown as weekly moving averages from 12 (‘Artega’) and 8 (‘Nagano’, ‘Nesbitt’, and ‘Trirosso’) plants. The average root mean square error (RMSE; $t\cdot ha^{-1}\cdot d^{-1}$) of the models was calculated for these daily predicted fresh weight yields and observed yields. Arrows within figures indicate the peaks of fresh weight yields.

sweet pepper (Fig. 6). For tomato and cucumber, a relatively constant number of fruits can be harvested during each harvest time compared with that of sweet pepper. Additionally, their ripening periods are shorter than those of sweet pepper (Adams et al. 2001; Marcelis 1994). Therefore, the daily dry matter fraction of tomatoes and cucumbers fruits was relatively constant compared with that of sweet peppers (Heuvelink 1997; Marcelis 1996). Simulation studies by Kang et al. (2011) and Marcelis (1994) partly supported this explanation. Therefore, crops with low fluctuations in fruit set, low strength of fruit sink, and a short period of fruit ripening may be characterized by stable dry matter partitioning to fruits during cultivation.

Table 3. Predicted and observed cumulative fresh weight yields of four sweet pepper cultivars grown in the greenhouse at the end of cultivation.

CV	DAT	Cumulative fresh wt yields ($t\cdot ha^{-1}$)		
		Model 1	Model 2	Observation
AT	250	110	136	135 ± 24 ⁱ
NG	244	111	113	112 ± 13
NS	244	124	120	101 ± 22
TR	244	86	93	90 ± 16

ⁱ Values are mean ± SD (AT: n = 12; TR: n = 8; NS: n = 8; NG: n = 8).

AT = Artega; CV = cultivar; DAT = days after transplanting; NG = Nagano; NS = Nesbitt; TR = Trirosso.

Unlike tomato and cucumber, fresh weight yields of sweet pepper significantly fluctuated during this study (Fig. 6). Daily dry matter partitioning to fruits also cyclically fluctuated during cultivation (Homma et al. 2022, 2024). The peaks and troughs of fresh weight yields were accurately predicted for model 2, but not for model 1, during this experiment. Both models used the same equations to estimate TDM_m (Eqs. [1] to [3]) and FWY_m (Eq. [5]). Therefore, the difference in predicted yield changes

Table 4. Average of the cumulative daily average air temperatures from anthesis to harvest ($^{\circ}C\cdot d$) calculated every 50 d for the four sweet pepper cultivars grown in the greenhouse.

DAT	Cumulative air temp until harvest after anthesis ($^{\circ}C\cdot d$) ⁱ			
	AT	NG	NS	TR
51–100	1240 ± 63 ⁱⁱ a ⁱⁱⁱ	1300 ± 53 a	1305 ± 87 a	1320 ± 67 a
101–150	1202 ± 100 a	1268 ± 99 a	1280 ± 119 a	1305 ± 112 a
151–200	1103 ± 125 b	1201 ± 108 b	1201 ± 100 b	1214 ± 109 b
201–250	1080 ± 115 b	1135 ± 84 c	1149 ± 68 c	1165 ± 207 b
Average	1125 ± 126	1197 ± 111	1198 ± 106	1225 ± 165

ⁱ Cumulative air temperatures were calculated by accumulating the daily average air temperatures from anthesis to harvest.

ⁱⁱ Values are presented as mean ± SD (AT: n = 341; TR: n = 269; NS: n = 132; NG: n = 126).

ⁱⁱⁱ Different letters indicate significant differences ($P < 0.05$ according to Tukey’s multiple comparison test).

AT = Artega; CV = cultivar; DAT = days after transplanting; NG = Nagano; NS = Nesbitt; TR = Trirosso.

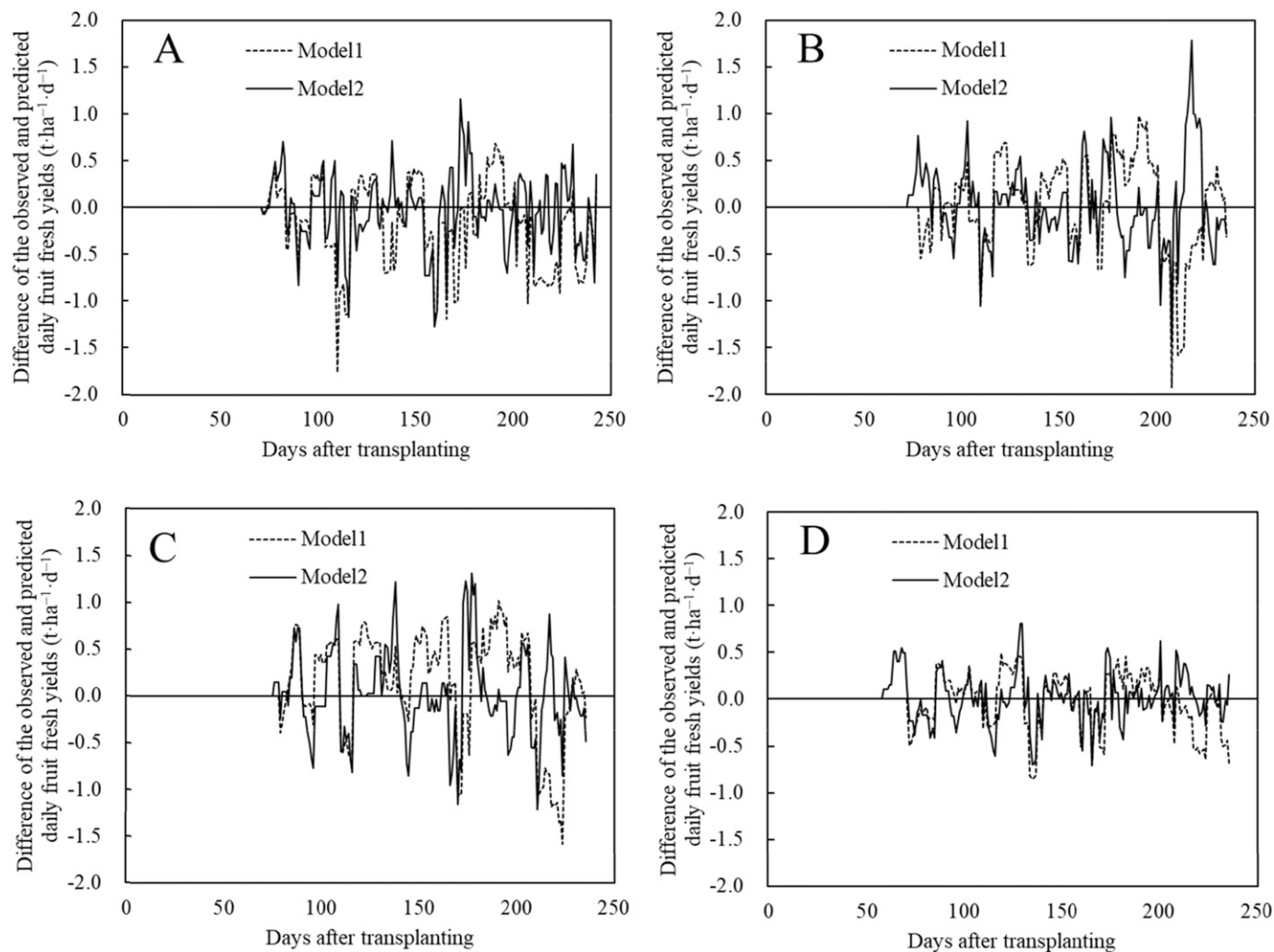


Fig. 7. Changes in differences between the observed and predicted (model 1: dashed line; model 2: solid line) daily fresh weight yields ($\text{t}\cdot\text{ha}^{-1}\cdot\text{d}^{-1}$) of four sweet pepper cultivars grown in the greenhouse from 0 to 250 d after transplanting. (A) 'Artega'. (B) 'Nagano'. (C) 'Nesbitt'. (D) 'Trirosso'. Observed fresh weight yields are shown as weekly moving averages from 12 ('Artega') and 8 ('Nagano', 'Nesbitt', and 'Trirosso') plants.

between model 1 and model 2 (Table 3, Fig. 6) resulted from different calculations of daily dry matter partitioning to fruits (model 1, Eq. [4]; model 2, Eqs. [6] to [12]). Therefore, the proposed sub-model (Eqs. [6] to [12]) in this study succeeded in imitating dry matter partitioning to the fruit organs. Introducing the sub-model (Eqs. [6] to [12]) into yield prediction models will be a promising approach for crops with high fluctuations in fruit set, high strength of fruit sink, and long periods of fruit ripening.

During this experiment, 'Trirosso' (Fig. 2) showed small fluctuations in fruit set (Fig. 4), fresh weight yields (Fig. 6), and dry matter partitioning to fruits on a daily basis (data not shown). These characteristics were approximately similar to those of tomato and cucumber (Heuvelink 1997; Marcelis 1996). Cultivars with a small fruit size ('Trirosso') had a high and stable fruit set with a low growth rate of fruits; therefore, daily dry matter partitioning to fruits might become relatively stable. These findings indicate that sweet pepper cultivars characterized by a small fruit size and fruit growth rate (e.g., 'Trirosso') (Fig. 2) showed less fluctuations in fresh weight yields, similar to tomato and cucumber. Overall, fresh weight yields were accurately predicted using model 1 for 'Trirosso' (Table 3, Fig. 6), tomato (Saito et al. 2020), and cucumber (Maeda and Ahn 2021).

In conventional practice, mature fruits are harvested every few days at production sites. More frequent harvest at the peaks of yield fluctuations may be recommended because daily harvestable fruits at the production site are limited by the working labor or the ability of the fruit selector. However, frequent harvest at the valleys of yield fluctuations may not be recommended because of the small number of harvestable fruits. Therefore, determining the number of harvests based on the amount of fresh weight yields may be effective for improving production efficiency. Additionally, succession planting based on the interval of flush may be effective for stable fruit production, as mentioned by Heuvelink et al. (2004). Overlapping the peaks and valleys of flush during the same period may be an effective approach to achieve stable fruit production.

During this experiment, cumulative daily average air temperature values after anthesis until harvest (CT, $^{\circ}\text{C}\cdot\text{d}$) fluctuated between 100 and 160 $^{\circ}\text{C}\cdot\text{d}$ (Table 4). Therefore, when plants are grown at daily average air temperatures of 20 to 21 $^{\circ}\text{C}$ (desired air temperatures for sweet pepper plant) (Bakker and van Uffelen 1988), the harvest period fluctuates by 5 to 8 d. Therefore, some fruits were harvested before and after the predicted harvest date during this experiment ('Artega', 160 DAT; 'Nagano', 100 DAT;

and 'Nesbitt', 140 DAT) (Fig. 6). Additionally, CT significantly decreased approximately 150 °C·d when comparing the periods between 51 and 100 DAT and 201 and 250 DAT (Table 4). This decrease resulted in misprediction of the harvest date and the prediction accuracy (Figs. 6 and 7). As previously reported, the speed of fruit growth is closely related to the temperature of fruits (Adams et al. 2001), and the surface temperature of tomato fruits becomes higher than the ambient air temperature when fruits are exposed to strong direct irradiance (Helyes et al. 2007). During this study, we observed a significant negative correlation between the average outside solar radiation from anthesis until harvest and the CT (data not shown). Similarly, the decrease in CT during cultivation may be partly related to environmental conditions. Elucidating the environmental factors that affect CT may be promising for increasing the accuracy of such prediction models.

The presented model may indicate underpredictions when plants are grown with severe environmental conditions. For example, the growth of sweet pepper is generally hampered under severe conditions, such as high and low temperatures, lack of irrigation, and high and low EC in a nutrient solution (Bosland and Votava 2012; de Souza et al. 2019; Erickson and Markhart 2002; Tadesse et al. 1999). Therefore, the range of environmental variables presented in this study is the premise for the robustness of the proposed model. Nevertheless, greenhouse sweet pepper usually grows in optimal environments and achieves high fresh weight yields. Therefore, we considered that the model presented here (Eqs. [1] to [3] and Eqs. [5] to [12]) showed sufficient prediction accuracy for practical applications.

The presented model showed accurate prediction using cultivar-specific parameters, such as the light extinction coefficient (*k*) and fruit dry matter content (Cd). Using these parameters is effective for predicting fresh fruit weight yields (Fig. 6); however, obtaining these parameters requires long-term experiments, as mentioned during this study. Therefore, we consider that the applicability of this model is still narrow. Obtaining the parameters presented here for wide ranges of cultivars may be necessary to increase applicability for growers. When applying our presented model at the production site, monitoring flower anthesis, or predicting the fruit set, incorporating the weather forecast into the presented model may help ease predictions.

In conclusion, our presented model showed high prediction accuracy for the fresh weight yields of sweet pepper, regardless of cultivar differences and fruit sizes. The fluctuations in fresh weight yields were predicted to follow a trend similar to the observed trends. Therefore, by obtaining coefficients for estimating the production of the total dry matter and fruit growth curve of the cultivar scheduled to be cultivated, accurate predictions of the short-term yield changes of sweet pepper are possible.

References Cited

Abdel-Mawgoud AMR, El-Abd SO, Böhme M, Sassine YN, Abou-Hadid AF. 2008. Weekly fruit production of sweet pepper in relation to plant fruit load manipulation. *Acta Hort.* 779:439–446. <https://doi.org/10.17660/ActaHortic.2008.779.55>.
 Adams SR, Cockshull KE, Cave CRJ. 2001. Effect of temperature on the growth and development of tomato fruits. *Ann Bot.* 88(5):869–887. <https://doi.org/10.1006/anbo.2001.1524>.
 Al-Halimi R, Moussa M. 2015. Long-term yield prediction of greenhouse sweet pepper crops. *GSTF J Agric Eng.* 2:2. <https://doi.org/10.7603/s40872-015-0002-7>.

Bakker JC, van Uffelen JAM. 1988. The effects of diurnal temperature regimes on growth and yield of glasshouse sweet pepper. *Neth J Agric Sci.* 36(3):201–208. <https://doi.org/10.18174/njas.v36i3.16670>.
 Bosland PW, Votava EJ. 2012. *Peppers: Vegetable and spice capsicums* (2nd ed). CABI, Wallingford, UK.
 de Souza AHC, Rezende R, Lorenzoni MZ, Santos FAS, de Oliveira JM. 2019. Response of bell pepper to water replacement levels and irrigation times. *Pesqui Agropecu Trop.* 49:1–7. <https://doi.org/10.1590/1983-40632019v49i3662>.
 Erickson AN, Markhart AH. 2002. Flower developmental stage and organ sensitivity of bell pepper (*Capsicum annuum* L.) to elevated temperature. *Plant Cell Environ.* 25:123–130. <https://doi.org/10.1046/j.0016-8025.2001.00807.x>.
 Helyes L, Lugasi A, Pek Z. 2007. Effect of natural light on surface temperature and lycopene content of vine ripened tomato fruit. *Can J Plant Sci.* 87(4):927–929. <https://doi.org/10.4141/CJPS07022>.
 Heuvelink E. 1996. Dry matter partitioning in tomato: Validation of a dynamic simulation model. *Ann Bot.* 77(1):71–80. <https://doi.org/10.1006/anbo.1996.0009>.
 Heuvelink E. 1997. Effect of fruit load on dry matter partitioning in tomato. *Scientia Hort.* 69(1–2):51–59. [https://doi.org/10.1016/S0304-4238\(96\)00993-4](https://doi.org/10.1016/S0304-4238(96)00993-4).
 Heuvelink E, Marcelis LFM, Korner O. 2004. How to reduce yield fluctuations in sweet pepper? *Acta Hort.* 633:349–355. <https://doi.org/10.17660/ActaHortic.2004.633.42>.
 Heuvelink E, Marcelis LFM, Kuerkels T. 2015. Young fruits pull so hard, flowers above abort: Developing fruits function too strongly as sink, p 18–19. In: Heuvelink E, Kuerkels T (eds). *Plant physiology in greenhouses*. Horti-Text BV, Woerden, the Netherlands.
 Higashide T. 2009. Prediction of tomato yield on the basis of solar radiation before anthesis under warm greenhouse conditions. *HortScience.* 44(7):1874–1878. <https://doi.org/10.21273/HORTSCI.44.7.1874>.
 Higashide T. 2018. Review of dry matter production and light interception by plants for yield improvement of greenhouse tomatoes in Japan. *Engeigaku Kenkyuu.* 17(2):133–146. <https://doi.org/10.2503/hrj.17.133>.
 Higashide T. 2022. Review of dry matter production and growth modelling for yield improvement of greenhouse tomatoes. *Hortic J.* 91(3):247–266. <https://doi.org/10.2503/hortj.UTD-R019>.
 Homma M, Watabe T, Ahn DH, Higashide T. 2022. Dry matter production and fruit sink strength affect fruit set ratio in a greenhouse sweet pepper. *J Am Soc Hortic Sci.* 147(5):270–280. <https://doi.org/10.21273/JASHS05228-22>.
 Homma M, Ahn DH, Higashide T. 2024. Effect of different fruit size and dry matter production on fruit load and fruit set ratio in a greenhouse sweet pepper. *Engeigaku Kenkyuu*. (In press).
 Hoshi T, Yasuba K, Kurosaki H, Okayasu T. 2018. Ubiquitous environment control system: An internet-of-things-based decentralized autonomous measurement and control system for a greenhouse environment, p 107–123. In: Hussmann S (ed). *Automation in agriculture*. InTechOpen, London, UK.
 Kang MZ, Yang LL, Zhang BG, de Reffye P. 2011. Correlation between dynamic tomato fruit-set and source-sink ratio: A common relationship for different plant densities and seasons? *Ann Bot.* 107(5):805–815. <https://doi.org/10.1093/aob/mcq244>.
 Lin WC, Hill BD. 2008. Neural network modelling to predict weekly yields of sweet peppers in a commercial greenhouse. *Can J Plant Sci.* 88(3):531–536. <https://doi.org/10.4141/cjps07165>.
 Lin WC, Frey D, Nigh GD, Ying CC. 2009. Combined analysis to characterize yield pattern of greenhouse-grown red sweet peppers. *HortScience.* 44(2):362–365. <https://doi.org/10.21273/HORTSCI.44.2.362>.
 Ma YT, Wubs AM, Mathieu A, Heuvelink E, Zhu JY, Hu BG, Cournepe PH, de Reffye P. 2011. Simulation of fruit-set and trophic competition and optimization of yield advantages in six *Capsicum* cultivars using functional-structural plant modelling. *Ann Bot.* 107(5):793–803. <https://doi.org/10.1093/aob/mcq223>.

- Maeda K, Ahn DH. 2021. Estimation of dry matter production and yield prediction in greenhouse cucumber without destructive measurements. *Agriculture*. 11(12):1186. <https://doi.org/10.3390/agriculture11121186>.
- Marcelis LFM. 1994. A simulation model for dry matter partitioning in cucumber. *Ann Bot*. 74(1):43–52. <https://doi.org/10.1006/anbo.1994.1092>.
- Marcelis LFM. 1996. Sink strength as a determinant of dry matter partitioning in the whole plant. *J Expt Bot*. 47:1281–1291. https://doi.org/10.1093/jxb/47.Special_Issue.1281.
- Marcelis LFM, Heuvelink E, Goudriaan J. 1998. Modelling biomass production and yield of horticultural crops: A review. *Scientia Hort*. 74(1–2):83–111. [https://doi.org/10.1016/S0304-4238\(98\)00083-1](https://doi.org/10.1016/S0304-4238(98)00083-1).
- Marcelis LFM, Elings A, Bakker M, Brajeul E, Dieleman A, De Visser PHB, Heuvelink E. 2006. Modelling dry matter production and partitioning in sweet pepper. *Acta Hort*. 718:121–128. <https://doi.org/10.17660/ActaHortic.2006.718.13>.
- Monsi M, Saeki T. 2005. On the factor light in plant communities and its importance for matter production. *Ann Bot*. 95(3):549–567. <https://doi.org/10.1093/aob/mci052>.
- Ohtani Y. 1997. Effective radiation, micrometeorological phenomena, p 106–107. In: Maki T, Iwata S, Uchijima Z, Oikawa T, Omasa K, Kurata K, Kozai T, Goto E, Kon EH, Nouchi I, Harazono Y, Hoshi T, Honjo H, Yamakawa S (eds). *Agricultural meteorology glossary* (in Japanese). Society for Agricultural Meteorology of Japan, Tokyo, Japan.
- R Core Team. 2020. R-3.6.3 for Windows. R Foundation for Statistical Computing, Vienna, Austria. <https://cran.r-project.org/bin/windows/base/old/3.6.3/>.
- Saito T, Kawasaki Y, Ahn DH, Ohshima A, Higashide T. 2020. Prediction and improvement of yield and dry matter production based on modeling and non-destructive measurement in year-round greenhouse tomatoes. *Hortic J*. 89(4):425–431. <https://doi.org/10.2503/hortj.UTD-170>.
- Sauviller C, Baets W, Verlinden B, Nicolai BM. 2009. Predicting the weekly yield fluctuations of greenhouse bell pepper. *Acta Hort*. 817:261–268. <https://doi.org/10.17660/ActaHortic.2009.817.27>.
- Tadesse T, Nichols MA, Fisher KJ. 1999. Nutrient conductivity effects on sweet pepper plants grown using a nutrient film technique: 1. Yield and fruit quality. *N Z J Crop Hortic Sci*. 27(3):229–237. <https://doi.org/10.1080/01140671.1999.9514101>.
- Tijskens LMM, Schouten RE, Lin WC. 2004. Predicting harvest labour allocation in bell pepper production. *Acta Hort*. 682:1435–1442. <https://doi.org/10.17660/ActaHortic.2005.682.192>.
- Verlinden BE, Nicolai BM, Sauviller C, Baets W. 2005. Bell pepper production prediction based on color development distribution, solar radiation and glass house temperature data. *Acta Hort*. 674:375–380. <https://doi.org/10.17660/ActaHortic.2005.674.46>.
- Watabe T, Homma M, Ahn DH, Higashide T. 2021. Examination of yield components and the relationship between dry matter production and fruit yield in greenhouse sweet pepper (*Capsicum annuum*). *Hortic J*. 90(3):247–254. <https://doi.org/10.2503/hortj.UTD-263>.
- Wien HC, Tripp KE, Hernandez-Armenta R, Turner AD. 1989. Abscission of reproductive structures in pepper: Causes, mechanisms and control, p 150–165. In: Green SK (ed). *Tomato and pepper production in the tropics*. R.O.C: Asian vegetable research and development center, Taipei, Taiwan.
- Wubs AM. 2010. Towards stochastic simulation of crop yield: A case study of fruit set in sweet pepper (PhD Diss). Wageningen Univ., Wageningen, The Netherlands.
- Wubs AM, Heuvelink E, Marcelis LFM. 2009a. Abortion of reproductive organs in sweet pepper (*Capsicum annuum* L.): A review. *J Hort Sci Biotechnol*. 84(5):467–475. <https://doi.org/10.1080/14620316.2009.11512550>.
- Wubs AM, Ma YT, Hemerik L, Heuvelink E. 2009b. Fruit set and yield patterns in six *Capsicum* cultivars. *HortScience*. 44(5):1296–1301. <https://doi.org/10.21273/HORTSCI.44.5.1296>.
- Wubs AM, Heuvelink E, Marcelis LFM, Hemerik L. 2011. Quantifying abortion rates of reproductive organs and effects of contributing factors using time-to-event analysis. *Funct Plant Biol*. 38(5):431–440. <https://doi.org/10.1071/FP10249>.
- Wubs AM, Ma YT, Heuvelink E, Hemerik L, Marcelis LFM. 2012. Model selection for nondestructive quantification of fruit growth in pepper. *J Am Soc Hortic Sci*. 137(2):71–79. <https://doi.org/10.21273/JASHS.137.2.71>.
- Yoshioka H, Takahashi K, Arai K, Nagaoka M. 1977. Studies on the translocation and accumulation of photosynthates in fruit vegetables, 1. Effect of the night- and root-temperatures with light intensities and nitrogen levels on the translocation and distribution of ¹⁴C-photosynthates in Tomato plants. *Bull Veg Ornamental Crops Res Stn*. A3:31–41.